Available online at www.sciencedirect.com

SCIENCE DIRECT

ELSEVIER

Genomics 85 (2005) 462–471

GENOMICS

www.elsevier.com/locate/ygeno

Identification and characterization of multiple isoforms of a murine and human tumor suppressor, *patched*, having distinct first exons☆

Kazuaki Nagao[a], Masashi Toyoda[a], Kaori Takeuchi-Inoue[a], Katsunori Fujii[b], Masao Yamada[a], Toshiyuki Miyashita[a,*]

[a]*Department of Genetics, National Research Institute for Child Health and Development, 2-10-1 Ohkura, Setagaya-ku, Tokyo 157-8535, Japan*
[b]*Department of Pediatrics, Graduate School of Medicine, Chiba University, 1-8-1 Inohana, Chuo-ku, Chiba 260-8670, Japan*

Received 3 September 2004; accepted 23 November 2004
Available online 11 January 2005

Abstract

Mutations in mouse and human *patched* (*PTCH*) genes are associated with birth defects and cancer. PTCH, a 12-pass transmembrane protein, is a receptor for Sonic hedgehog (Shh) signaling proteins. Shh proteins activate transcription of target genes, including *PTCH*, via GLI transcription factors. Here we identified seven and five isoforms of human and mouse *PTCH* mRNA, respectively, which are generated by the complex alternative use of five exons as the first exon (exons 1a to 1e in the 5′-to-3′ order). Although expression profiles of these isoforms were highly variable among human tissues, three of them, *PTCHa*, *PTCHb*, and *PTCHd*, were predominantly expressed in most tissues, *PTCHd* being most ubiquitous. In contrast, *PTCHb* was always predominant and reached a maximum at E10.5 during mouse development. These three mRNA isoforms encode three PTCH proteins with distinct N-termini, $PTCH_L$, $PTCH_M$, and $PTCH_S$. The expression of these three isoforms was regulated by GLI transcription factors, and at least two functional GLI-binding sequences were identified, one in exon 1a and the other between exon 1a and exon 1b. $PTCH_L$ and $PTCH_M$ were equally active in terms of suppressing GLI-mediated transcription and inducing apoptosis. $PTCH_S$ protein (encoded by *PTCHd*), lacking the first transmembrane domain, was more unstable than the other two, resulting in a reduced activity. This study may shed light on the mechanism whereby a single *PTCH* gene plays a role in both tumor cell growth and embryonic development.

Keywords: *Patched*; Sonic hedgehog; Basal cell carcinoma; Medulloblastoma; Alternative splicing

The Sonic hedgehog (Shh) signaling cascade is pivotal to embryonic development, because holoprosencephaly (HPE), characterized by a failure of the forebrain to separate completely into hemispheres, and HPE-like abnormalities are associated with a loss of Shh function in humans and in mice [1–3]. The role of the Shh pathway in tumorigenesis was also established with the discovery that inactivating mutations in the *Patched* (*PTCH*) gene, which encodes one component of the Shh receptor, are responsible for the inherited cancer predisposition disorder known as Gorlin's or nevoid basal cell carcinoma syndrome (NBCCS) [4,5], as well as sporadic basal cell carcinomas (BCCs) and medulloblastomas [6–8]. NBCCS is an autosomal dominant neurocutaneous disorder characterized by developmental abnormalities such as palmar and plantar pits, jaw cysts, calcification of the falx cerebri, and skeletal anomalies and also by a predisposition to cancers such as BCC and medulloblastoma [9]. Familial and sporadic BCCs display loss of heterozygosity in this region, consistent with *PTCH* being a tumor suppressor gene [6,10]. In addition, activating mutations in *Smoothened* (*Smo*), also encoding another component of the Shh receptor, have been detected in BCCs [11], further emphasizing the importance of this pathway in tumor development. More importantly, the recent finding that this pathway is essential for growth of a wide range of tumor types not associated with NBCCS, such as lung

☆ Sequence data from this article have been deposited with the GenBank Library under Accession Nos. AB164615, AB164616, and AB189436–AB189442.

* Corresponding author. Fax: +81 3 5494 7035.
E-mail address: tmiyashita@nch.go.jp (T. Miyashita).

0888-7543/$ - see front matter © 2004 Elsevier Inc. All rights reserved.
doi:10.1016/j.ygeno.2004.11.014

cancers or digestive tract tumors, sheds light on potential new diagnostic and therapeutic approaches [12–14].

PTCH, a 12-pass transmembrane protein, is the ligand-binding component of the Shh receptor complex. In the absence of Shh binding, PTCH is thought to hold Smo, a 7-pass transmembrane protein, in an inactive state and thus inhibit signaling to downstream genes. Upon the binding of Shh, the inhibition of Smo is released and signaling is transduced, leading to the activation of target genes by the Gli family of transcription factors [15]. The transcription of *PTCH* itself is induced by Shh pathway activity [16], thus generating a negative feedback loop, which may play an important role in tumor suppression by inhibiting a sustained activation of the pathway.

Hahn et al. predicted that there are three different forms of the PTCH protein present in humans: the ancestral form and two human-specific forms [4]. Recently, a detailed characterization of three alternative first exons was reported [17]. However, our study using the 5′ rapid amplification of cDNA ends (5′RACE) technique revealed the existence of an additional first exon and unexpectedly complex splicing between the first and the second exons that is evolutionarily conserved across species. Therefore, the characterization of several potential forms of the PTCH protein may reveal the mechanism whereby a single *PTCH* gene could play a role in different pathways, and the determination of the regulation of different splice forms of *PTCH* mRNA may shed light on the apparent role of the gene in tumor cell growth as well as embryonic development. Here we characterize multiple isoforms of *PTCH* in humans and mice and discuss the functions of their products, expression profiles, and transcriptional regulation.

Results

Isolation of isoforms of human and mouse PTCH

PTCH is a multiexon gene comprising 23 exons distributed over a region of ~70 kb. To date, three cDNA sequences encoding the human *PTCH* gene's first exon have been reported and named exons 1, 1A, and 1B [17], and another exon has recently been deposited with GenBank (exon 1a described below, GenBank Accession No. BC043542). In contrast, only a single mRNA species of *PTCH* has been reported in mice [18] (GenBank Accession No. U46155). Due to the use of alternative exons, several mRNA isoforms are generated. On the basis of this background we performed a comprehensive analysis of the 5′ structure of mRNA species derived from the human *PTCH* gene employing the 5′RACE technique. Sequencing of 31 RACE clones revealed an additional alternative first exon (exon 1c described below, submitted to GenBank as Accession No. AB189438) and complex splicing between the first and the second exon. Using a genomic sequence containing the *PTCH* gene (GenBank Accession No. AL161729), the precise genomic organization of the human *PTCH* gene was determined as shown in Fig. 1. For the sake

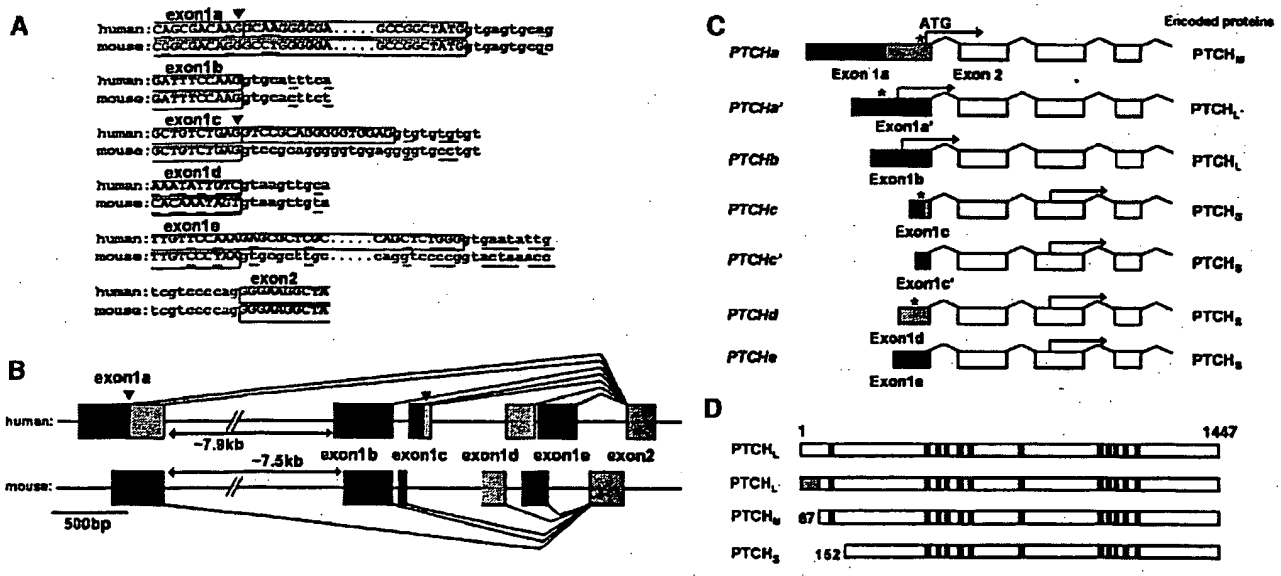

Fig. 1. Identification of human and mouse *PTCH* isoforms. (A) Comparison of human and mouse exon–intron boundaries. Upper- and lowercase letters indicate exon and intron sequences, respectively. Nucleotides not conserved between the two species are underlined. Alternative splice donor sites are indicated by arrowheads. (B) 5′ region of human and mouse *PTCH* gene structure. The 5′ ends of the mouse first exons have not been determined. (C) 5′ structure of *PTCH* isoforms. The positions of the first methionine codons and in-frame stop codons are indicated by arrows and asterisks, respectively. In four of seven mRNAs, in-frame stop codons were identified. The first in-frame methionine codon could be determined in the other three transcripts since the 5′RACE system we employed amplifies only full-length transcripts [47]. (D) PTCH protein isoforms encoded by mRNA species described in (C). Numbers refer to amino acid positions relative to the first methionine of $PTCH_L$. The positions of the 12 transmembrane regions are indicated by filled boxes. $PTCH_{L'}$ has 65 unique amino acid residues at the N-terminus depicted with a shaded box.

of simplicity, we named the first exons exon 1a to 1e on the basis of their 5′-to-3′ order. Thus, exons 1b, 1d, and 1e are the former exons 1B, 1, and 1A, respectively. In addition to multiple first exons, we found that alternative 5′ splice sites allow the shortening of exons 1a and 1c, generating exons 1a′ and 1c′ (Fig. 1C). The complex alternative splicing described above thus generates up to seven mRNA species, each with its own distinct 5′ sequence (Figs. 1B and 1C). RT-PCR using isoform-specific forward primers for each alternative exon 1 and a common reverse primer for exon 2 indeed validated the existence of the seven different mRNAs. These mRNA isoforms encode four PTCH proteins termed $PTCH_L$, $PTCH_{L'}$, $PTCH_M$, and $PTCH_S$ (Figs. 1C and 1D). $PTCH_S$ is an N-terminally truncated PTCH protein that lacks the first transmembrane domain (Fig. 1D). Although only a single species of *PTCH* mRNA has been reported in mice, a comparison of the human *PTCH* genomic sequence with the mouse sequence (NCBI Locus NT_039587) suggested the existence of multiple first exons. In this study, mouse and human *Patched* genes are collectively referred to by the human nomenclature (*PTCH*, whereas mouse *Patched* is often called *Ptc*). RT-PCR using the forward primers constructed at mouse putative first exons and reverse primers at exon 2 demonstrated that most of the *PTCH* isoforms found in humans are indeed conserved in mice. At least in mouse P19 cells and several mouse tissues from which total RNA was extracted, *PTCHa′* and *PTCHc* have not been identified and the splice donor site at exon 1e was different from that of humans (Fig. 1A). All exons were flanked by splice junctions that conformed to the consensus GT–rule except for exon 1a′–exon 2 in humans, in which the GC–AG intron was observed. GC–AG introns are occasionally found and processed by the same splicing pathway as conventional GT–AG introns [19].

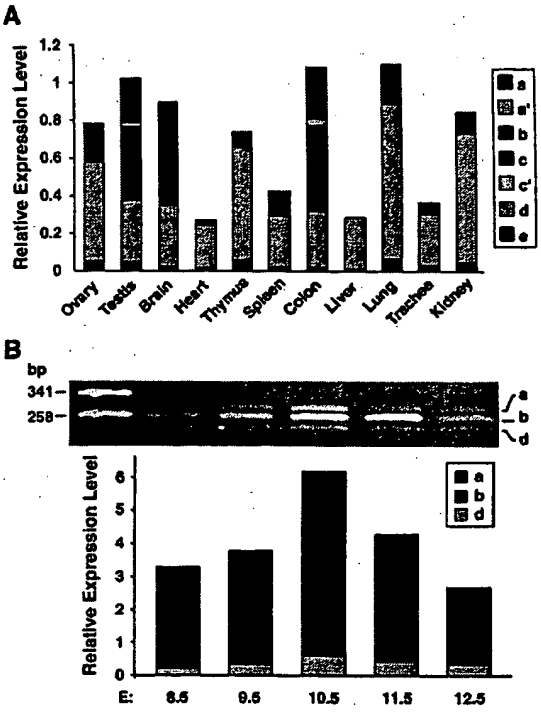

Fig. 2. Expression profiling of *PTCH* isoforms. (A) RT-PCR analysis of expression profiles in various tissues. Total RNA obtained from a panel of human tissues was subjected to RT-PCR. Forward primers specific to each of the first exons and a common reverse primer for exon 2 were synthesized and used for PCR. The RT-PCR products were quantified with an Agilent 2100 bioanalyzer. *PTCH* expression levels were normalized to those of *GAPDH*. Exons with relative expression levels lower than 0.007 do not appear in the graph. (B) RT-PCR analysis of expression profiles in various mouse developmental stages. Total RNA obtained from mouse embryos at various developmental stages was subjected to RT-PCR using mouse-specific primers. Mean *PTCH* expression levels normalized to β-*actin* expression are presented at the bottom (n = 2–4).

Expression profiles of three isoforms of PTCH in various tissues

Selective usage of the 5′-most exons suggests a complex tissue-specific transcriptional regulation. Therefore, to investigate the expression profiles of *PTCH* isoforms, RT-PCR was performed with isoform-specific primers for the first alternative exons using total RNA from a panel of human tissues, and profiles were analyzed with an Agilent 2100 bioanalyzer. As shown in Fig. 2A, *PTCH* was expressed in a wide range of human tissues. However, the levels of total *PTCH* RNA varied among human tissues. For example, the heart and liver showed low levels of expression, which is largely consistent with previous reports on human and mouse *PTCH* expression [18,20]. Expression profiles of the *PTCH* isoforms were also highly variable among tissues. While *PTCHd* (encoding $PTCH_S$) was widely expressed, the expression of *PTCHa* (encoding $PTCH_M$) and *PTCHb* (encoding $PTCH_L$) was relatively restricted. For example, *PTCHb* was expressed in all the analyzed tissues apart from liver, while the expression of *PTCHa* was more restricted, showing virtually no expression in the heart, thymus, liver, and trachea. The other *PTCH* isoforms using exons 1a′, 1c, 1c′, and 1e were found to be expressed at very low levels if at all throughout the tissues. Therefore, we focused on *PTCHa*, *PTCHb*, and *PTCHd* in further experiments. Since Shh signaling plays a key role in embryonic development, we next investigated the expression profile in mouse embryogenesis. Consistent with a previous report, the expression of *PTCH* reached a maximum at E10.5, at which point the limb buds become increasingly prominent, and declined thereafter [18]. Notably, in contrast to human adult tissues, the expression of *PTCHb* was always prevalent during embryonic development (Fig. 2B).

Transcriptional regulation of PTCH isoforms by GLI

It is well known that *PTCH* itself is one of the target genes in the Shh signaling network creating a negative feedback loop and a balance via the antagonism of Shh and

PTCH. Even though the GLI proteins may well not be the only mediators of Shh signaling, the overwhelming majority of available data on insects and vertebrates indicates a central role for GLI proteins in regulating the mediation and interpretation of Shh signals. As shown in Fig. 3, the expression of all three *PTCH* isoforms was elevated by GLI1 in the cell lines we employed. However, a closer observation revealed slight differences in the degree of induction. For example, *PTCHd* and *PTCHb* were more strongly upregulated by GLI1 in 293T and HSC-2 cells, whereas the induction of *PTCHa* was more evident than that of *PTCHb* or *PTCHd* in Ho-1-u-1 and LK-2 cells, indicating cell type-specific regulation of the isoforms.

PTCH promoter has functional GLI-binding sites

The *Drosophila patched* gene (*ptc*) has a cluster of three GLI consensus binding sites (5′-TGGGTGGTC-3′ or 5′-GACCACCCA-3′) [21] in the promoter region that is required for the reporter gene expression in response to Hedgehog (Hh) activity [22]. Recently, it was reported that the transcriptional regulation of *PTCH* by Shh signaling was mediated by a single GLI-binding site located ~400 bp upstream of exon 1b (GLI-BS1 in Fig. 4A) [23]. However, sequencing farther upstream indicated the presence of even two more consensus GLI-binding sequences not reported previously (GLI-BS2 and GLI-BS3 in Fig. 4A, −3965 and −8283 bp relative to the reported transcription start site of exon 1b, respectively). The mouse upstream sequence also contained three putative consensus GLI-binding sites and

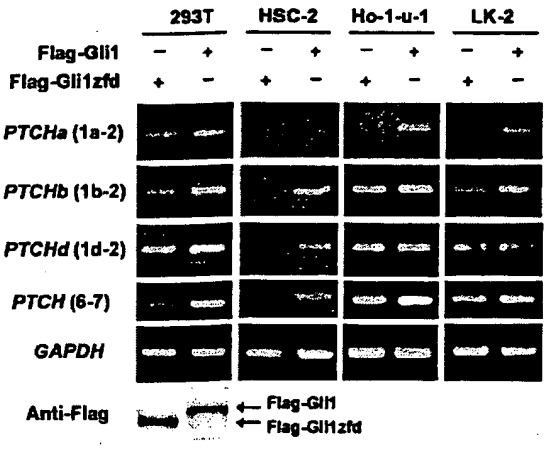

Fig. 3. Transcriptional regulation of three *PTCH* isoforms. Cell lines indicated at the top were transfected with the expression plasmid pSRα-Flag-Gli1 or pSRα-Flag-Gli1zfd. pSRα-Flag-Gli1zfd is a plasmid for a mutant GLI1 lacking the zinc finger domain [43] used as a negative control for pSRα-Flag-Gli1. Cells were cultured in 0.5% FCS for 16 h after the transfection and total RNA was extracted from the transfected cells and subjected to RT-PCR. Forward and reverse primers were constructed for the exons indicated in parentheses. PTCH (6–7) indicates the overall *PTCH* expression because exons 6 and 7 are used regardless of the isoform. The expression of Flag-tagged GLI1 proteins was confirmed by immunoblotting using anti-Flag antibody (Anti-Flag).

the sequences around these sites were strikingly conserved (Fig. 4B). This suggests that two upstream consensus GLI-binding sequences, as well as a reported one, act as GLI-responsive elements. To test this assumption, genome fragments containing GLI-BS1, GLI-BS2, and GLI-BS3 were inserted into a luciferase construct (pGV-PTCH1, pGV-PTCH2, and pGV-PTCH3, respectively). Cotransfection of the GLI1 expression plasmid with pGV-PTCH1 enhanced the luciferase activity in SH-SY5Y cells (Fig. 4C), confirming a previous report. In addition, as anticipated, GLI1 expression also enhanced the luciferase activity when cotransfected with reporter constructs containing upstream GLI-binding sequences (pGV-PTCH2 and pGV-PTCH3). To confirm that these sites are really responsible for the GLI-mediated activation, a mutation with four nucleotide substitutions was introduced into GLI-binding sequences (5′-T*AGTGGA*TC-3′ or 5′-GA*TCCACTA*-3′, mutated nucleotides in italic), generating the constructs pGV-PTCH1mt, pGV-PTCH2mt, and pGV-PTCH3mt. The introduction of these mutations into the putative GLI-binding sites indeed abolished the elevation of luciferase activity induced by GLI1. Furthermore, the 1.1-kb mouse fragment containing GLI-BS1 showed a similar response to GLI1 expression (pGV-mPTCH) (Fig. 4C), suggesting that the mechanism by which *PTCH* expression is regulated by the Shh signaling pathway is conserved.

We also examined whether GLI protein could physically associate with putative GLI-binding elements in *PTCH* in vitro and in vivo. First, we tested these sites in an electrophoretic mobility shift assay. As shown in Fig. 4D, when GST–GLI3 fusion protein was incubated with a wild-type DNA probe containing a putative GLI consensus sequence in the promoter region, a complex with a shift in gel mobility was detected (lane 3). In contrast, substitution of GST nonfusion for GST–GLI3, or mutant DNA probe with the same nucleotide substitutions as described above for the wild-type sequence, resulted in a failure to detect a complex whose mobility was altered in these assays (lanes 2 and 6). Moreover, the DNA–protein complex was abolished by competition with an unlabeled oligonucleotide containing the GLI site, but not by a mutated oligonucleotide, demonstrating the specificity of the complex formation (lanes 4 and 5). GST–GLI3 also bound specifically to two more upstream sequences with a GLI-binding consensus sequence (lanes 9 and 15) in vitro.

To determine whether the GLI protein occupies these sites in vivo, we used a chromatin immunoprecipitation (ChIP) assay to analyze lysates extracted from 293T cells transfected with a plasmid to express Flag–GLI1. The genomic fragments including GLI-BS1 and GLI-BS3 were specifically precipitated as a GLI–DNA complex with an anti-Flag antibody (Fig. 4E, lanes 3 and 11), while GLI-BS2 was barely coimmunoprecipitated (lane 7). As controls, the same fragments were not precipitated when cells were transfected with a construct for Flag tag or the lysates were incubated with an anti-Myc antibody (lanes 2, 4, 10, and

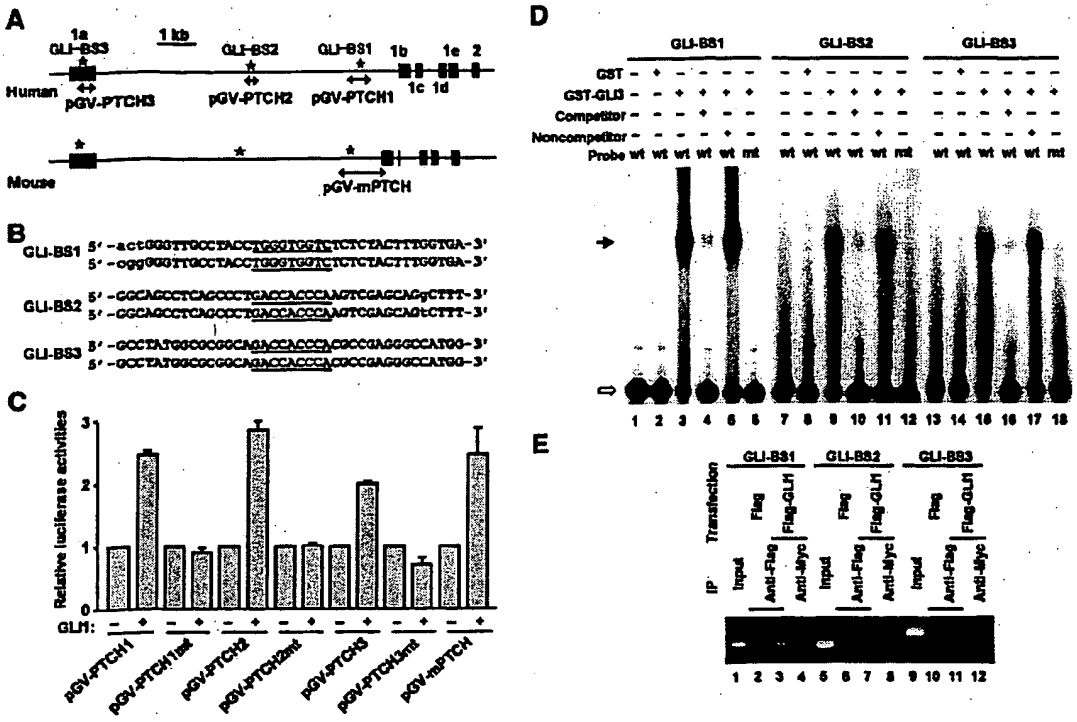

Fig. 4. Transcriptional regulation of *PTCH* isoforms. (A) Comparison of human and mouse genomic structures. Black boxes indicate locations and relative sizes of exons. Asterisks indicate the positions of three putative GLI-binding sequences (5′-TGGGTGGTC-3′ or 5′-GACCACCCA-3′). DNA fragments inserted into luciferase vectors to make the reporter gene constructs are indicated by arrows. The names of the resulting constructs are indicated below. (B) Comparison of human (top) and mouse (bottom) GLI-binding sequences. Consensus GLI-binding sequences are underlined. Lowercase letters indicate nucleotides not conserved between the two species. (C) The *PTCH* promoter is GLI responsive. SH-SY5Y cells were cotransfected with various reporter gene constructs as indicated with or without pSRα-Flag-GLI1. Cells were cultured in 0.5% FCS for 16 h after the transfection and then harvested for the luciferase assay. Firefly luciferase activity was normalized by *Renilla* luciferase activity from a cotransfected pRL-SV40 and is indicated relative to the activity of the same reporter without pSRα-Flag-GLI1. The total amount of transfected DNA was adjusted using pcDNA3.0. Data are representative of three experiments with similar results. (D) GLI protein can bind in vitro to an oligonucleotide probe representing the *PTCH* gene region. Recombinant GST or GST–GLI3 protein was incubated with ^{32}P-labeled oligonucleotide DNA probes containing a putative GLI-consensus sequence (wt) or a mutated version with four nucleotide substitutions (mt), together with or without a 50-fold molar excess of cold competitor containing the GLI site (competitor) or its mutant (noncompetitor). DNA–protein complexes were size fractionated in a nondenaturing polyacrylamide gel and were detected by autoradiography. The positions of the free probe and the shifted complexes are indicated by the open and closed arrows, respectively. (E) Identification of GLI-binding region in vivo. ChIP assay was performed with genomic fragments including the putative GLI-binding consensus sequence indicated at the top. Chromatin from 293T cells transfected with pCI-Flag (lanes 2, 6, 10) or pFlag-GLI1 (lanes 3, 4, 7, 8, 11, 12) was immunoprecipitated with anti-Flag antibody (lanes 2, 3, 6, 7, 10, 11). PCR amplification was performed with corresponding templates. Input represents a portion of the sonicated chromatin before immunoprecipitation. Anti-Myc antibody was used as a negative control (lanes 4, 8, 12).

12). Taken together, our data show that at least GLI-BS1 and GLI-BS3 are involved in GLI-mediated *PTCH* expression. In contrast, GLI-BS2 is not accessible to GLI in vivo, probably due to a higher genomic structure, although the accessibility may be cell-type dependent.

Functional analysis of three isoforms of PTCH

In 293T cells, overexpression of PTCH protein causes apoptosis and inhibition of cell proliferation [24,25]. Thus, it is expected that there is a basal level of leakage activity of Smo that excess PTCH prevents in the apparent absence of Shh. The fact that cyclopamine has a proapoptotic effect in these cells supports this possibility (discussed below). On the basis of this background, we performed a functional analysis of the PTCH isoforms using a GLI-responsive luciferase reporter in 293T cells. Luciferase activities were suppressed when 293T cells were transfected with plasmids for $PTCH_L$ and $PTCH_M$ but not with an empty vector, pcDNA3.0 (Fig. 5A). This suppression was not observed when cells were transfected with the plasmid for *PTCHΔC* which encodes only 194 N-terminal amino acid residues, indicating the specificity of the results. To investigate the function of PTCH in vivo, PTCH was transiently expressed in 293T cells. As expected, $PTCH_L$ and $PTCH_M$ induced apoptosis in 293T cells as measured by assessing the sub-G0/G1 population (Fig. 5B). However, they were not as potent as cyclopamine, a well-known inhibitor of Shh signaling [26]. This is probably, at least in part, due to the presence of untransfected cells. Interestingly, in contrast to $PTCH_L$ and $PTCH_M$, $PTCH_S$ did not significantly suppress GLI-responsive luciferase activity or induce apoptosis, implying that this isoform does not have the expected function of a PTCH protein or the expression level of this isoform

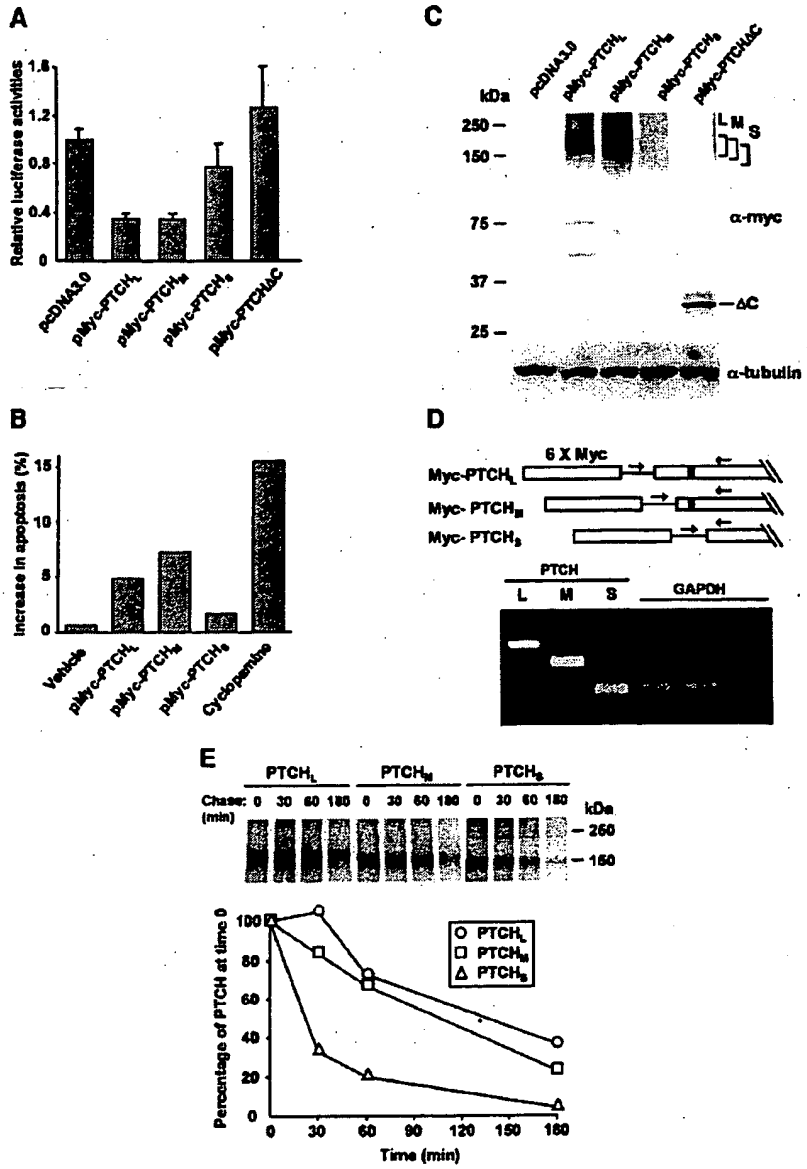

Fig. 5. Functional analysis of PTCH isoforms. (A) Inhibition of GLI-responsive luciferase activity by PTCH. 293T cells were transfected with various expression plasmids as indicated together with 8 × GLI-Luc containing eight GLI-binding sites and LTR-LacZ. After the transfection, cells were cultured in 0.5% FCS for 16 h and then harvested for the luciferase assay. Firefly luciferase activity was normalized to β-galactosidase activity from a cotransfected LTR-lacZ vector. Data are representative of three experiments with similar results. (B) PTCH-induced cell death as measured based on DNA content. 293T cells were transfected with plasmids for PTCH or treated with cyclopamine or vehicle alone (ethanol). The induction of apoptosis was assessed by the increase in the subG0/G1 population compared with mock-transfected cells. (C) Protein levels of expressed genes. Cell lysates were obtained from 293T cells transfected with indicated plasmids and subjected to immunoblotting with an anti-c-Myc antibody. Tubulin is a loading control. The molecular weights of the four PTCH protein products predicted from the composition of amino acid residues, including the Myc tag, are as follows: $PTCH_L$, 172 kDa; $PTCH_M$, 163 kDa; $PTCH_S$, 154 kDa; PTCHΔC, 32.2 kDa. (D) RT-PCR analysis of expressed genes. Total RNA was extracted from 293T cells transfected with plasmids for each isoform of *PTCH* and RT-PCR analysis was performed using primers depicted at the top. A forward primer was constructed in the linker region between the Myc tag and *PTCH* and a reverse primer in exon 2. Filled boxes indicate the position of the first transmembrane domain. GAPDH is an internal control for RT-PCR. (E) Metabolic labeling of the PTCH proteins. 293T cells transfected with a construct for PTCH were pulse-labeled with [^{35}S]methionine and chased for the indicated periods. ^{35}S-labeled PTCH was immunoprecipitated, detected by autoradiography (top), and then quantified by phosphorimaging. Levels of labeled PTCH are plotted relative to the amount present at time 0 (bottom).

is too low to cause these changes. To examine these possibilities, we first investigated the protein levels of each PTCH isoform by immunoblotting. Compared with $PTCH_L$, $PTCH_M$, and PTCHΔC, the protein level of $PTCH_S$ was markedly reduced (Fig. 5C). The diffuse migration of PTCH proteins is thought to be due to glycosylation as reported [27,28]. However, when RT-PCR was performed to analyze mRNA levels, these three isoforms were found to be expressed at comparable levels (Fig. 5D). These results indicate that the stability of $PTCH_S$ protein is compromised.

To determine whether the reduced activity of $PTCH_S$ was due to decreased protein stability, we measured the half-life of the three isoforms. 293T cells transfected with a plasmid for each isoform were metabolically labeled with [^{35}S]-methionine and then incubated with excess unlabeled amino acids for various lengths of time. PTCH proteins were immunoprecipitated and size-separated by SDS–PAGE. As shown in Fig. 5E, Myc-tagged PTCH proteins were visualized at a point corresponding to approximately the same size as that detected by immunoblotting. Following a 180-min chase, 36 and 23% of de novo synthesized $PTCH_L$ and $PTCH_M$, respectively, remained in 293T cells. Half-lives were calculated as 115 and 83 min, respectively. In contrast, the degradation of $PTCH_S$ was considerably accelerated, such that 5% of the protein remained at 180 min (half-life 26 min). These results indicated that $PTCH_S$ is an unstable protein compared with $PTCH_L$ and $PTCH_M$.

Discussion

Alternative pre-mRNA splicing is an important mechanism for generating protein diversity and may explain in part how mammalian complexity arises from a surprisingly small complement of genes. It also plays important roles in development and disease. A recent study estimated that greater than 55% of human genes are alternatively spliced [29] and that about 10% of the mutations in the human genome affect the canonical splice site sequence [30]. In particular, isoforms of genes with alternative first exons may have distinct mechanisms of expression. For example, the *DSCR1* (Down syndrome candidate region 1)/*MCIP1* (modulatory calcineurin-interacting protein 1) and *nNOS* (neuronal nitric oxide synthase) genes have four and eight alternative first exons, respectively, and are subjected to a distinct expressional regulation by separate promoters [31,32].

In this study, we identified and characterized five alternative first exons in both human and mouse *PTCH* genes encoding four protein species. Thus, arguably, *PTCH* is one of the most complex human genes in terms of diversity at the 5′ end. The transcription of all major isoforms was upregulated by GLI1, an upstream transcription factor in the Shh pathway, although the degree of activation was cell type-specific. Unlike *Drosophila ptc* in which only a single transcript has been reported and whose promoter has a cluster of three GLI-binding consensus sequences in a 130-bp region [22], human and mouse *PTCH* have three consensus sequences dispersed over 7.5 kb between exon 1a and exon 1b (Fig. 4A). Since exons 1b, 1c, 1d, and 1e are located close to each other, it is likely that *PTCH* isoforms except *PTCHa* are regulated by at least partially overlapping promoters, including GLI-BS1 in Fig. 4A. In contrast, exon 1a is located ~8 kb upstream of exon 1b and one of the GLI-binding sites is located inside exon 1a and the other two are located far downstream. No GLI-binding consensus sequence was found in the promoter region of *PTCHa* (i.e., upstream of exon 1a), at least not up to the 40 kb position. Thus, taking our results with the ChIP assay into consideration, it is likely that the two GLI-binding sequences, one in exon 1a and the other far downstream of exon 1a (GLI-BS3 and GLI-BS1 in Fig. 4A, respectively), are responsible for the GLI-mediated regulation of *PTCHa*. This is not unexpected because *hepatocyte nuclear factor-3β*, another target gene of Shh signaling, has a GLI-binding site 3′ of the transcription unit and this site is essential for the response to Shh [33]. Although NBCCS families who show linkage to chromosomal regions other than 9q22.3–q31, to where *PTCH* has been mapped, have not been reported, a considerable number of NBCCS patients do not have mutations within the coding region of *PTCH* [34–36]. Therefore, taking our results into account, it is warranted to examine mutations in GLI-binding sequences using samples from such patients. Interestingly, *PTCH2*, another homologue of the *Drosophila Hh* gene, whose mutations are found in BCC and medulloblastoma [37], also has a GLI-binding consensus sequence ~470 bp upstream of the first methionine codon (based on the genomic sequence, AL136380), indicating that *PTCH2* is another target gene of the Shh pathway. Supporting this notion, PTCH2 is upregulated in basal cell carcinoma in which Shh signaling is activated [38].

$PTCH_L$ and $PTCH_M$ were equally potent in terms of suppressing GLI-mediated transcription or inducing apoptosis. In contrast, the $PTCH_S$ protein was less potent due to its instability. Amino acid residues 101–119 of $PTCH_L$ and 35–53 of $PTCH_M$ comprise the first transmembrane domain, which is absent in $PTCH_S$ because it starts with Met^{152} in $PTCH_L$ (Fig. 1D). This probably explains why $PTCH_S$ is unstable. However, $PTCH_S$ was more ubiquitously expressed throughout adult tissues than the other two, implying that, despite its instability, $PTCH_S$ may be important for tissue homeostasis or tumor suppression. It is possible that a certain extracellular stress or stimulus such as the binding of Shh may stabilize $PTCH_S$. In contrast, the expression of $PTCH_L$ was always predominant during embryonic development, indicating that $PTCH_L$ plays a key role in embryogenesis.

The generation of mice in which one of the isoforms is nonfunctional may help clarify the roles of the alternative proteins in normal development and carcinogenesis. In this study, we focused on the usage of alternative first exons. However, some cell-surface receptors, such as CD44, undergo a complex, combinatorial splicing that determines the function of the gene products [39]. Although the major transcripts of human and mouse *PTCH* are ~8 kb long [18,20], we have identified rare transcripts lacking exons 4 and 5 (K.N. and T.M., unpublished data). Therefore, a comprehensive study of alternative pre-mRNA splicing throughout the gene using cost-effective and high-throughput methods, such as polymerase colony technology [40] or

exon junction microarrays [41], may shed light on the functional complexity of the *PTCH* gene and carcinogenesis with increased Shh pathway activity.

Materials and methods

Isolation of human PTCH isoforms and construction of plasmids

To obtain 5′ ends of cDNA, RNA ligase-mediated 5′RACE was performed using the GeneRacer kit (Invitrogen) according to the manufacturer's directions. Random primers were used to reverse transcribe RNA. A reverse gene-specific primer was constructed in exon 2 to amplify the first-strand cDNA. The amplified cDNA was subcloned into pCR4-TOPO (Invitrogen) and sequenced. The expression plasmid encoding Myc-tagged $PTCH_L$ (pMyc-Ptc1) was kindly provided by Dr. Jeffrey Ming. To make expression plasmids for $PTCH_M$ and $PTCH_S$, a DNA fragment encoding the N-terminal region of $PTCH_L$ was excised from pMyc-Ptc1 by digestion with *Eco*RI and replaced with the RT-PCR product encoding the N-terminal region of $PTCH_M$ or $PTCH_S$, respectively. To make luciferase constructs, pGV-PTCH1, pGV-PTCH2, and pGV-PTCH3, fragments for the human *PTCH* promoter ranging from bp −1354 to −746, −4105 to −3808, and −8427 to −8032, respectively, relative to the reported transcription start site (GenBank Accession No. NM_000264) were subcloned into pGV-P2 (Wako Chemicals, Osaka, Japan). Mutated plasmids for these constructs were created by PCR-mediated mutagenesis as described previously [42]. The authenticity of all constructs was confirmed by DNA sequencing. The expression vector for FLAG-GLI1, pSRα-Flag-GLI1 [43], and the reporter vector, 8 × GLI-Luc [33], were kindly provided by Dr. Alexander L. Joyner and Hiroshi Sasaki, respectively.

Cell culture and transfections

The human embryonic kidney cell line 293T and mouse embryonal carcinoma cell line P19 were maintained in DMEM supplemented with 10% fetal calf serum (FCS), 50 U/ml penicillin, and 0.1 mg/ml streptomycin at 37°C in a humidified atmosphere of 5% CO_2. The human neuroblastoma line SH-SY5Y, oral squamous cell carcinoma lines HSC-2 and Ho-1-u-1, and lung squamous cell carcinoma line LK-2 (obtained from Cell Resource Center for Biomedical Research, Tohoku University, Japan) were maintained similarly except that RPMI 1640 medium was used. Cells were transfected with the indicated plasmids using Effectene reagent (Qiagen) and harvested at 16 h after the lipofection.

Analysis of PTCH isoform expression profiles

Human and mouse *PTCH* cDNA was amplified by RT-PCR using 0.5 μg of total RNA purified from a panel of human tissues (Ambion and Clontech) or mouse embryos and primers 5′-CTGGGAGAAGACGGAGGA-GC-3′ (exon 1a forward, human), 5′-CCCGGGAAATTA-ATAAAAGG-3′ (exon 1a forward, mouse), 5′-GGACCG-GGACTATCTGCACC-3′ (exon 1b forward, human), 5′-GGACCGGGACTATCTGCACC-3′ (exon 1b forward, mouse), 5′-CCTCTCCAGGAAAAGCAGCA-3′ (exon 1c forward, human), 5′-GAGAAAGCAGCAGACAAGT-GAAGGTTG-3′ (exon 1c forward, mouse), 5′-ATCC-ATGTGGCTGCCCTCTT-3′ (exon 1d forward, human), 5′-ATCCTTGTGGCCGCCCTCTT-3′ (exon 1d forward, mouse), 5′-TTCTCGGCGGG-GGTCCAGTT-3′ (exon 1e forward, human), 5′-CCAGA-TGGACCACGGTTGCTG-TAGATT-3′ (exon 1e forward, mouse), 5′-CACAGCTC-CTCCACGTTGGT-3′ (exon 2 reverse, human), and 5′-CA-CAGCTCCTCCACGTTGGT-3′ (exon 2 reverse, mouse). During the log phase of amplification (25–35 cycles depending on the templates), 1 μl of the PCR product was applied onto a DNA LabChip (Agilent Technologies) and loaded into an Agilent 2100 bioanalyzer according to the manufacturer's protocol. Data analysis was performed with Agilent 2100 bioanalyzer software. The expression of *PTCH* was normalized to that of the glyceraldehyde-3-phosphate dehydrogenas (*GAPDH*) gene or β-actin gene.

Western blotting

Immunoblot analysis was performed as described previously [44]. In brief, 30 μg of the cell lysate was subjected to SDS–PAGE and transferred onto a nitrocellulose membrane. The membrane was incubated with anti-c-Myc (Santa Cruz, 9E10) or anti-Flag (Sigma, M2) mouse monoclonal antibody followed by horseradish peroxidase-conjugated anti-mouse immunoglobulins (DAKO). The proteins were visualized using enhanced chemiluminescence immunoblotting detection reagents (Amersham).

Luciferase assay

293T or SH-SY5Y cells growing on six-well culture plates were cotransfected using Effectene reagent with various combinations of plasmids as indicated in the figure legends. Transfected cells were maintained in 0.5% FCS for 16 h and then harvested for the luciferase assay using the reagents and protocols provided by Promega or Wako chemicals.

Electrophoretic mobility shift assay

To obtain GST–GLI3 fusion protein, *Escherichia coli* strain BL21(DE3)pLysS (Novagen) was transformed with pGST-GLI3MF [45] (a gift from Dr. Shunsuke Ishii), which encodes the metal finger region of GLI3. The fusion protein was purified by affinity chromatography using glutathione–Sepharose 4B (Amersham Pharmacia Biotech) according to the manufacturer's instructions. The ^{32}P-labeled double-stranded oligonucleotide probes containing the sequence

for a consensus GLI-binding site (5′-TTGCCTACCTGGGTGGTCTCTCTACTT-3′, 5′-CTCAGCCCTGACCACCCAAGTCGAGCA-3′, and 5′-GGCGCGGCAGACCACCCACGCCGAGGG-3′) or a mutated sequence (5′-TTGCCTACCT*AGTGGA*TCTCTCTACTT-3′, 5′-CTCAGCCCTGA*TCCACTA*AGTCGAGCA-3′, and 5′-GGCGCGGCAGA*TCCACTA*CGCCGAGGG-3′) (mutated nucleotides in italic) were incubated with the GST or GST–GLI3 fusion (200 ng). The reaction was performed in 10 μl of binding buffer containing 4% glycerol, 1 mM $MgCl_2$, 0.5 mM EDTA, 50 mM NaCl, 10 mM Tris–HCl (pH 7.5), and 0.05 mg/ml poly(dI–dC) for 20 min at room temperature. For competition experiments, a 50-fold molar excess of unlabeled, double-stranded oligonucleotide, containing either a GLI site or a mutated GLI site as described above, was included in binding reactions. Samples were fractionated on a nondenaturing 6% polyacrylamide gel and visualized by autoradiography.

Apoptosis assay

293T cells were plated at 4×10^5 per well onto a six-well plate, grown for 16 h, transfected with plasmids for Myc-tagged PTCH or treated with cyclopamine (Toronto Research Chemicals, Inc.) (5 μM final concentration), and then grown in DMEM with 0.5% FCS. After 24 h, relative DNA content was determined by flow cytometry as described previously [46]. Cells having a reduced DNA content (sub-G0/G1) were regarded as apoptotic.

Pulse–chase experiment

293 cells were plated at 8×10^5 cells per 60-mm plate, cultured for 24 h, and transfected with 1 μg of PTCH expression plasmid using the Lipofectamine Plus reagent kit (Invitrogen) according to the manufacturer's instructions. Twenty-four hours after the transfection, cells were incubated with DMEM lacking methionine (−Met) for 30 min and then with 16.7 μCi/ml of L-[^{35}S]methionine with DMEM − Met for 2 h. Cells were washed three times with phosphate-buffered saline (PBS) and incubated with DMEM supplemented with 2 mM methionine for varying periods. At each time point, cells were scraped, washed with PBS, and lysed in 300 μl of lysis buffer containing 150 mM NaCl, 1% Triton X-100, 10 mM Tris–HCl (pH 7.4), 5 mM EDTA, 1 mM PMSF, 18 μg/ml aprotinin, 50 μg/ml leupeptin, 1 mM benzamidine, and 0.7 μg/ml pepstatin. The extracts were pelleted at 16,000*g* for 15 min at 4°C, and the supernatants (200 μl) were immunoprecipitated for 16 h with 20 μl of protein–A/G agarose (Santa Cruz) and 3 μl of anti-c-Myc antibody. The immunoprecipitates were washed three times with 1 ml of lysis buffer, solubilized in 20 μl of 1 × Laemmli buffer by heating at 95°C for 5 min, and resolved on a 5–20% gradient polyacrylamide gel. Gels were dried, exposed, and analyzed using a FUJIX BAS2000 imaging analyzer (Fuji Film).

ChIP assay

ChIP assay was performed using the acetyl-histone H3 ChIP Assay Kit (Upstate Biotechnology), as recommended by the manufacturer, except that monoclonal anti-Flag (M2) and anti-Myc antibodies (9E10) were used in this study. 293T cells were plated at 1×10^6 cells per 10-cm dish, grown for 16 h, and then transfected with pFlag-Gli1 or pCI-Flag (encoding Flag-tag epitope). After 24 h, genomic DNA and protein were cross-linked by addition of formaldehyde (1% final concentration) directly to the culture medium and incubated for 10 min at 37°C. Cells were lysed in 1 ml of SDS lysis buffer containing 1% SDS, 10 mM EDTA, and 50 mM Tris–HCl (pH 8.1) and sonicated to generate 300- to 1000-bp DNA fragments. After centrifugation, the cleared supernatant was diluted 10-fold with ChIP dilution buffer and incubated with the specific antibody at 4°C for 16 h with rotation before incubation with protein A–Sepharose beads at 4°C for 1 h with rotation. Immune complexes were precipitated, washed, and eluted as recommended. DNA–protein cross-links were reversed by heating to 65°C for 2.5 h. DNA was phenol extracted, ethanol precipitated, and resuspended in 20 μl of Tris–EDTA. We used 2.5 μl of each sample as a template for PCR. PCR amplification was performed using primers that flank the putative GLI-response elements, 5′-AAAGGCTGGAGCTCCCGCCC-3′ (GLI-BS1, forward) and 5′-TGCGCGCAAAGGCATCCCAC-3′ (GLI-BS1, reverse), or 5′-GGGCATGCATATTAAAGCCG-3′ (GLI-BS2, forward) and 5′-CGAGCGCTATCTTAATCTCC-3′ (GLI-BS2, reverse), or 5′-AGCGCCTGTTTACCCAGGAG-3′ (GLI-BS3, forward) and 5′-GCTCCTCCGTCTTCTCCCAG-3′ (GLI-BS3, reverse).

Acknowledgments

We thank Mayu Yamazaki for technical support, Kayoko Saito for preparing the manuscript, and Drs. J. Ming (Children's Hospital of Philadelphia), A. Joyner (NYU Medical Center), S. Ishii (Tsukuba Life Science Center, RIKEN), and H. Sasaki (Center for Developmental Biology, RIKEN) for providing plasmids. This work was supported by Grants for Brain Research, Cancer Research, Genome Research, and Child Health and Development from the Ministry of Health, Labor, and Welfare, and a Grant-in-Aid for Scientific Research and the Budget for Nuclear Research from the Ministry of Education, Culture, Sports, Science, and Technology of Japan.

References

[1] E. Belloni, et al., Identification of *Sonic hedgehog* as a candidate gene responsible for holoprosencephaly, Nat. Genet. 14 (1996) 353–356.
[2] E. Roessler, et al., Mutations in the human *Sonic hedgehog* gene cause holoprosencephaly, Nat. Genet. 14 (1996) 357–360.

[3] C. Chiang, et al., Cyclopia and defective axial patterning in mice lacking *Sonic hedgehog* gene function, Nature 383 (1996) 407–431.
[4] H. Hahn, et al., Mutations of the human homolog of Drosophila *patched* in the nevoid basal cell carcinoma syndrome, Cell 85 (1996) 841–851.
[5] R.L. Johnson, et al., Human homolog of *patched*, a candidate gene for the basal cell nevus syndrome, Science 272 (1996) 1668–1671.
[6] A.B. Unden, et al., Mutations in the human homologue of *Drosophila patched* (*PTCH*) in basal cell carcinomas and the Gorlin syndrome: different *in vivo* mechanisms of PTCH inactivation, Cancer Res. 56 (1996) 4562–4565.
[7] C. Raffel, et al., Sporadic medulloblastomas contain *PTCH* mutations, Cancer Res. 57 (1997) 842–845.
[8] T. Pietsch, et al., Medulloblastomas of the desmoplastic variant carry mutations of the human homologue of Drosophila patched, Cancer Res. 57 (1997) 2085–2088.
[9] R.J. Gorlin, Nevoid basal-cell carcinoma syndrome, Medicine 66 (1987) 98–113.
[10] M.R. Gailani, et al., The role of the human homologue of *Drosophila patched* in sporadic basal cell carcinomas, Nat. Genet. 14 (1996) 78–81.
[11] J. Xie, et al., Activating Smoothened mutations in sporadic basal-cell carcinoma, Nature 391 (1998) 90–92.
[12] S.P. Thayer, et al., Hedgehog is an early and late mediator of pancreatic cancer tumorigenesis, Nature 425 (2003) 851–856.
[13] D.M. Berman, et al., Widespread requirement for Hedgehog ligand stimulation in growth of digestive tract tumours, Nature 425 (2003) 846–851.
[14] D.N. Watkins, et al., Hedgehog signalling within airway epithelial progenitors and in small-cell lung cancer, Nature 422 (2003) 313–317.
[15] P.W. Ingham, A.P. McMahon, Hedgehog signaling in animal development: paradigms and principles, Genes Dev. 15 (2001) 3059–3087.
[16] D.M. Berman, Medulloblastoma growth inhibition by hedgehog pathway blockade, Science 297 (2002) 1559–1561.
[17] P. Kogerman, et al., Alternative first exons of *PTCH1* are differentially regulated *in vivo* and may confer different functions to the PTCH1 protein, Oncogene 21 (2002) 6007–6016.
[18] L.V. Goodrich, R.L. Johnson, L. Milenkovic, J.A. McMahon, M.P. Scott, Conservation of the hedgehog/patched signaling pathway from flies to mice: induction of a mouse patched gene by Hedgehog, Genes Dev. 10 (1996) 301–312.
[19] Q. Wu, A.R. Krainer, AT-AC pre-mRNA splicing mechanisms and conservation of minor introns in voltage-gated ion channel genes, Mol. Cell Biol. 19 (1999) 3225–3236.
[20] H. Hahn, et al., A mammalian *patched* homolog is expressed in target tissues of *sonic hedgehog* and maps to a region associated with developmental abnormalities, J. Biol. Chem. 271 (1996) 12125–12128.
[21] K.W. Kinzler, B. Vogelstein, The GLI gene encodes a nuclear protein which binds specific sequences in the human genome, Mol. Cell Biol. 10 (1990) 634–642.
[22] C. Alexandre, A. Jacinto, P.W. Ingham, Transcriptional activation of *hedgehog* target genes in *Drosophila* is mediated directly by the cubitus interruptus protein, a member of the GLI family of zinc finger DNA-binding proteins, Genes Dev. 10 (1996) 2003–2013.
[23] M. Ågren, P. Kogerman, M.I. Kleman, M. Wessling, R. Toftgård, Expression of the *PTCH1* tumor suppressor gene is regulated by alternative promoters and a single functional Gli-binding site, Gene 330 (2004) 101–114.
[24] E.A. Barnes, M. Kong, V. Ollendorff, D.J. Donoghue, Patched1 interacts with cyclin B1 to regulate cell cycle progression, EMBO J. 20 (2001) 2214–2223.
[25] C. Thibert, et al., Inhibition of neuroepithelial patched-induced apoptosis by sonic hedgehog, Science 301 (2003) 843–846.
[26] J.K. Chen, J. Taipale, M.K. Cooper, P.A. Beachy, Inhibition of Hedgehog signaling by direct binding of cyclopamine to Smoothened, Genes Dev. 16 (2002) 2743–2748.
[27] E.C. Bailey, L. Milenkovic, M.P. Scott, J.F. Collawn, R.L. Johnson, Several *PATCHED1* missense mutations display activity in *patched1*-deficient fibroblasts, J. Biol. Chem. 277 (2002) 33632–33640.
[28] V. Marigo, R.A. Davey, Y. Zuo, J.M. Cunningham, C.J. Tabin, Biochemical evidence that patched is the Hedgehog receptor, Nature 384 (1996) 176–179.
[29] Z. Kan, E.C. Rouchka, W.R. Gish, D.J. States, Gene structure prediction and alternative splicing analysis using genomically aligned ESTs, Genome Res. 11 (2001) 889–900.
[30] P.D. Stenson, et al., Human Gene Mutation Database (HGMD): 2003 update, Hum. Mutat. 21 (2003) 577–581.
[31] J.J. Fuentes, M.A. Pritchard, X. Estivill, Genomic organization, alternative splicing, and expression patterns of the *DSCR1* (Down syndrome candidate region 1) gene, Genomics 44 (1997) 358–361.
[32] Y. Wang, et al., RNA diversity has profound effects on the translation of neuronal nitric oxide synthase, Proc. Natl. Acad. Sci. U.S.A. 96 (1999) 12150–12155.
[33] H. Sasaki, C. Hui, M. Nakafuku, H. Kondoh, A binding site for Gli proteins is essential for *HNF-3β* floor plate enhancer activity in transgenics and can respond to Shh in vitro, Development 124 (1997) 1313–1322.
[34] K. Fujii, et al., Mutations in the human homologue of *Drosophila patched* in Japanese nevoid basal cell carcinoma syndrome patients, Hum. Mutat. 21 (2003) 451–452.
[35] A. Chidambaram, et al., Mutations in the human homologue of the Drosophila *patched* gene in Caucasian and African-American nevoid basal cell carcinoma syndrome patients, Cancer Res. 56 (1996) 4599–4601.
[36] C. Wicking, et al., Most germ-line mutations in the nevoid basal cell carcinoma syndrome lead to a premature termination of the PATCHED protein, and no genotype–phenotype correlations are evident, Am. J. Hum. Genet. 60 (1997) 21–26.
[37] I. Smyth, et al., Isolation and characterization of human *patched 2* (*PTCH2*), a putative tumour suppressor gene in basal cell carcinoma and medulloblastoma on chromosome 1p32, Hum. Mol. Genet. 8 (1999) 291–297.
[38] P.G. Zaphiropoulos, A.B. Undén, F. Rahnama, R.E. Hollingsworth, R. Toftgård, *PTCH2*, a novel human patched gene, undergoing alternative splicing and up-regulated in basal cell carcinomas, Cancer Res. 59 (1999) 787–792.
[39] J. Lesley, R. Hyan, CD44 structure and function, Front. Biosci. 3 (1998) D616–D630.
[40] J. Zhu, J. Shendure, R.D. Mitra, G.M. Church, Single molecule profiling of alternative pre-mRNA splicing, Science 301 (2003) 836–838.
[41] J.M. Johnson, et al., Genome-wide survey of human alternative pre-mRNA splicing with exon junction microarrays, Science 302 (2003) 2141–2144.
[42] Y. Imai, Y. Matsushima, T. Sugimura, M. Terada, A simple and rapid method for generating a deletion by PCR, Nucleic Acids Res. 19 (1991) 2785.
[43] H.L. Park, et al., Mouse *Gli1* mutants are viable but have defects in SHH signaling in combination with a *Gli2* mutation, Development 127 (2000) 1593–1605.
[44] T. Miyashita, Y. Okamura-Oho, Y. Mito, S. Nagafuchi, M. Yamada, Dentatorubral pallidoluysian atrophy (DRPLA) protein is cleaved by caspase-3 during apoptosis, J. Biol. Chem. 272 (1997) 29238–29242.
[45] P. Dai, et al., Sonic Hedgehog-induced activation of the *Gli1* promoter is mediated by GLI3, J. Biol. Chem. 274 (1999) 8143–8152.
[46] K. Fujii, et al., γ-Irradiation deregulates cell cycle control and apoptosis in nevoid basal cell carcinoma syndrome-derived cells, Jpn. J. Cancer Res. 90 (1999) 1351–1357.
[47] B.C. Schaefer, Revolutions in rapid amplification of cDNA ends: new strategies for polymerase chain reaction cloning of full-length cDNA ends, Anal. Biochem. 227 (1995) 255–273.